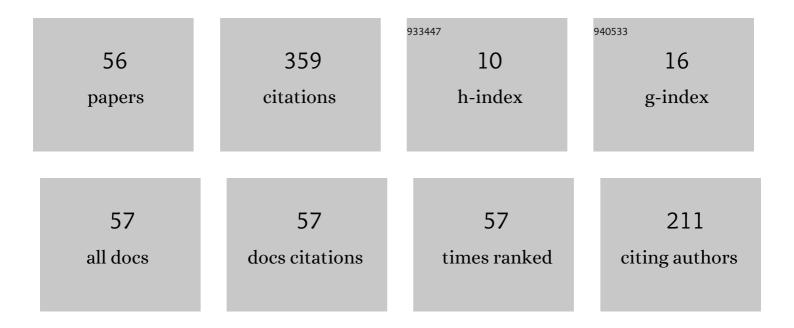
Valeriy Volodin

List of Publications by Year in descending order

Source: https://exaly.com/author-pdf/7236435/publications.pdf Version: 2024-02-01



#	Article	IF	CITATIONS
1	Ð~ЗВЛЕЧЕÐÐ~Е СЕЛЕÐЕÐ~З ПÐОМПÐОДУКТОВ МЕТÐЛЛУÐГÐ~ЧЕСКÐ Shikisattardy Keshendi Paidalanu, 2018, 307, 56-64.	žĐ"Đž ĐŸ† 8.2	Ð₽žÐ⁻ЗÐ
2	A new carbon structure in annealed film coatings of the carbon–lead system. Technical Physics Letters, 2017, 43, 126-129.	0.7	1
3	Melt–gas phase equilibria and state diagrams of the selenium–tellurium system. Russian Journal of Physical Chemistry A, 2017, 91, 800-804.	0.6	6
4	Study of the possibility of solving cosmological lithium problem in an accelerator experiment. Physics of Atomic Nuclei, 2017, 80, 203-210.	0.4	0
5	Interaction between 20â^'30 keV X-ray quanta and deuterated crystal structures. Journal of Surface Investigation, 2017, 11, 179-185.	0.5	4
6	Cluster Structure of ⁹ Be from ³ He+ ⁹ Be Reaction. Journal of Physics: Conference Series, 2016, 724, 012031.	0.4	10
7	New carbon structures in annealed carbon–cadmium film coatings. Journal of Surface Investigation, 2016, 10, 1187-1191.	0.5	1
8	Melt–vapor phase transition in the lead–selenium system at atmospheric and low pressure. Russian Journal of Physical Chemistry A, 2016, 90, 572-574.	0.6	1
9	Investigation of the reaction D(4He, γ)6Li at ultralow energies. Physics of Particles and Nuclei Letters, 2016, 13, 190-197.	0.4	2
10	Effect of pd and dd reactions enhancement in deuterides TiD2, ZrD2 and Ta2D in the astrophysical energy range. Physics of Particles and Nuclei Letters, 2016, 13, 79-97.	0.4	7
11	Structure and phase composition of deposited tantalum–carbon films. Physics of Metals and Metallography, 2016, 117, 789-794.	1.0	5
12	Phase diagram of the selenium–sulfur system in the pressure range 1 × 10–5–1 × 10–1 MPa. Russian Journal of Physical Chemistry A, 2016, 90, 2183-2187.	0.6	2
13	A method for investigation of the D(4He, γ)6Li reaction in the Ultralow energy region under a high background. Nuclear Instruments and Methods in Physics Research, Section A: Accelerators, Spectrometers, Detectors and Associated Equipment, 2016, 825, 24-30.	1.6	3
14	Targets of deuterides TiD2, ZrD2, NbD, and CrD2 with different structures used in experiments on the study of pd and dd reactions at astrophysical energies. Nuclear Instruments and Methods in Physics Research, Section A: Accelerators, Spectrometers, Detectors and Associated Equipment, 2016, 810, 80-85.	1.6	5
15	Textured targets of deuterides TiD2, ZrD2, NbD, and CrD2 in experiments to study the pd and dd reaction mechanisms at astrophysical energies. Physics of Particles and Nuclei Letters, 2016, 13, 98-103.	0.4	1
16	Cadmium telluride in tellurium—cadmium films consisting of ultradispersed particles. Technical Physics, 2015, 60, 1171-1175.	0.7	1
17	Structure and phase composition of films formed by ultradispersed particles of iron and carbon. Journal of Surface Investigation, 2015, 9, 822-830.	0.5	4
18	Formation of porous \hat{I}_{\pm} tantalum in films. Technical Physics, 2015, 60, 1157-1161.	0.7	3

VALERIY VOLODIN

#	Article	IF	CITATIONS
19	Tantalum-cadmium film coatings: Preparation, phase composition, and structure. Physics of Metals and Metallography, 2015, 116, 56-62.	1.0	9
20	Structure and phase composition of niobium-copper deposited films. Journal of Surface Investigation, 2015, 9, 178-183.	0.5	4
21	Whisker microcrystals on the surface of tantalum–cadmium alloy films. Technical Physics Letters, 2015, 41, 529-531.	0.7	9
22	Inelastic scattering and clusters transfer in 3,4He + 9Be reactions. Physics of Particles and Nuclei Letters, 2015, 12, 703-712.	0.4	13
23	Liquid-vapor phase equilibrium in a tin-selenium system. Russian Journal of Physical Chemistry A, 2014, 88, 2029-2034.	0.6	5
24	The structural-phase state of iron-carbon coatings formed by the ultradispersed particles. , 2014, , .		1
25	Structure of niobium-tungsten alloy films produced by metal sputtering. Journal of Surface Investigation, 2014, 8, 1146-1151.	0.5	1
26	Structure of \hat{l}^2 -tantalum-tungsten alloy films produced by the codeposition of sputtered metals. Journal of Surface Investigation, 2014, 8, 169-174.	0.5	4
27	First experimental evidence of D(p,γ)3He reaction in deuteride titanium in ultralow collision energy region. Nuclear Instruments and Methods in Physics Research, Section A: Accelerators, Spectrometers, Detectors and Associated Equipment, 2014, 753, 91-96.	1.6	10
28	Study of the d(p, γ)3He reaction at ultralow energies using a zirconium deuteride target. Nuclear Instruments and Methods in Physics Research, Section A: Accelerators, Spectrometers, Detectors and Associated Equipment, 2014, 737, 248-252.	1.6	13
29	Effect of the crystal structure of a deuterated target on the yield of neutrons in the dd reaction at ultralow energies. JETP Letters, 2014, 99, 497-502.	1.4	10
30	Radiation-induced phase transition in a film of niobium-tin solid solution. Technical Physics, 2014, 59, 1136-1140.	0.7	2
31	Experimental observation of electron screening for the D(p, \hat{I}^3)3He nuclear reaction in titanium Deuteride TiD. Physics of Particles and Nuclei Letters, 2014, 11, 467-472.	0.4	2
32	First experimental evidence of D(p, γ)3He reaction in titanium deuteride in ultralow collision energy region. Journal of Experimental and Theoretical Physics, 2014, 119, 54-62.	0.9	4
33	Experimental verification of hypothesis of dd reaction enhancement by channeling of deuterons in titanium deuteride at ultralow energies. Nuclear Instruments and Methods in Physics Research, Section A: Accelerators, Spectrometers, Detectors and Associated Equipment, 2014, 764, 42-47.	1.6	12
34	High-temperature decomposition of solid solutions of beta-tantalum with copper in films. Physics of Metals and Metallography, 2014, 115, 481-485.	1.0	0
35	New Mo3Pb phase with a15 structure formed in solid solutions of film molybdenum-lead system. Physics of Metals and Metallography, 2014, 115, 500-506.	1.0	7
36	Nanosize Î ² -tantalum coatings: Formation, structure, and properties. Physics of Metals and Metallography, 2013, 114, 573-579.	1.0	8

VALERIY VOLODIN

#	Article	IF	CITATIONS
37	Structure and phase composition of Nb-C deposited films. Physics of Metals and Metallography, 2013, 114, 395-399.	1.0	9
38	Amorphous silicon coatings with silver nanoparticles. Technical Physics Letters, 2013, 39, 998-1000.	0.7	3
39	Structure of sputter-deposited films of \hat{l}^2 -tantalum-aluminum alloys. Physics of Metals and Metallography, 2013, 114, 935-939.	1.0	5
40	Structural features of Ag-Cu alloy films produced by the codeposition of sputtered metals. Journal of Surface Investigation, 2013, 7, 1183-1187.	0.5	2
41	Measuring the astrophysical S factors and the cross sections of the p(d, γ)3He reaction in the ultralow energy region using a zirconium deuteride target. Physics of Particles and Nuclei Letters, 2013, 10, 717-722.	0.4	5
42	Investigation of temperature dependence of neutron yield and electron screening potential for the d(d, n)3He reaction proceeding in deuterides ZrD2 and TiD2. Physics of Atomic Nuclei, 2012, 75, 913-922.	0.4	17
43	Measurement of astrophysical S-factors and electron screening potentials for reaction in ZrD2, TiD2 and TaD0.5 targets in the ultralow energy region using plasma accelerator. Nuclear Physics A, 2012, 889, 93-104.	1.5	25
44	Measurement of astrophysical S factors and electron screening potentials for d(d, n)3He reaction In ZrD2, TiD2, D2O, and CD2 targets in the ultralow energy region using plasma accelerators. Physics of Atomic Nuclei, 2012, 75, 53-62.	0.4	11
45	Liquid-vapor phase transition in a stratifying lead-zinc system upon a reduction in pressure. Russian Journal of Physical Chemistry A, 2011, 85, 1285-1287.	0.6	1
46	Determining a liquidus line under isothermal conditions. Russian Journal of Physical Chemistry A, 2011, 85, 2047-2049.	0.6	0
47	Micro- and nanocomposite Ti-Al-N/Ni-Cr-B-Si-Fe-based protective coatings: Structure and properties. Technical Physics, 2011, 56, 1023-1030.	0.7	16
48	Experimental determination of the electron screening potential energy for the d(d, n)3He Reaction in ZrD2 and D2O in the ultralow energy region. Bulletin of the Russian Academy of Sciences: Physics, 2010, 74, 1570-1574.	0.6	2
49	Liquid-vapor phase equilibrium in the stratifying thallium-zinc system. Russian Journal of Non-Ferrous Metals, 2010, 51, 205-211.	0.6	2
50	Investigation of the structure and physicochemical properties of combined nanocomposite coatings based on Ti–N–Cr/Ni–Cr–B–Si–Fe. Russian Physics Journal, 2009, 52, 1317-1324.	0.4	12
51	Nanocomposite protective coatings based on Ti–N–Cr/Ni–Cr–B–Si–Fe, their structure and properties Vacuum, 2009, 83, S235-S239.	^{5.} 3.5	53
52	The thermodynamic properties of liquid and vapor in the cadmium-thallium-lead system. Russian Journal of Physical Chemistry A, 2009, 83, 1817-1822.	0.6	0
53	Liquid-vapor phase transition upon pressure decrease in the lead-bismuth system. Russian Journal of Physical Chemistry A, 2009, 83, 1993-1995.	0.6	1
54	Saturated vapor pressure in the thallium-cadmium system. Russian Journal of Physical Chemistry A, 2008, 82, 1075-1079.	0.6	4

#	Article	IF	CITATIONS
55	Novel superconducting niobium beryllide Nb3Be with A15 structure. JETP Letters, 2003, 78, 440-442.	1.4	18
56	Glancing angle X-ray diffractometry of ion-implanted metals by means of synchrotron radiation. Nuclear Instruments and Methods in Physics Research, Section A: Accelerators, Spectrometers, Detectors and Associated Equipment, 1991, 308, 308-311.	1.6	2